

Dynamics of a spherical minority game

T Galla[†], A C C Coolen[‡] and D Sherrington[†]

[†] Department of Physics, University of Oxford, Theoretical Physics, 1 Keble Road, Oxford OX1 3NP, UK

[‡] Department of Mathematics, King's College London, The Strand, London WC2R 2LS, UK

Abstract. We present an exact dynamical solution of a spherical version of the batch minority game (MG) with random external information. The control parameters in this model are the ratio of the number of possible values for the public information over the number of agents, and the radius of the spherical constraint on the microscopic degrees of freedom. We find a phase diagram with three phases: two without anomalous response (an oscillating versus a frozen state), and a further frozen phase with divergent integrated response. In contrast to standard MG versions, we can also calculate the volatility exactly. Our study reveals similarities between the spherical and the conventional MG, but also intriguing differences. Numerical simulations confirm our analytical results.

PACS numbers: 02.50.Le, 87.23.Ge, 05.70.Ln, 64.60.Ht

E-mail: galla@thphys.ox.ac.uk, tcoolen@mth.kcl.ac.uk, d.sherrington1@physics.oxford.ac.uk

1. Introduction

The dynamics of interacting agents is currently studied intensively, applying the ideas and techniques of equilibrium and non-equilibrium statistical mechanics. One of the models which has attracted particular attention is the so-called minority game (MG), introduced as a minimalist econophysics model for a financial market [1]. The players in the MG are traders who, at each round of the game, have to make one of two possible choices (e.g. buy or sell) in response to publicly available information. Each aims to make profit by making the opposite choice to the majority of agents. The interaction between agents is indirect: they cannot observe individual actions of others, but only the subsequent cumulative effect of all actions on the market. To determine their own trading actions, each agent holds a pool of strategies, assigned randomly before the start of the game and then kept fixed. These effectively act as look-up tables, mapping the observation of publicly available information onto a proposed trading action. In the versions of the MG studied so far (e.g. [1, 2, 3, 4]) agents cannot combine strategies, but select the one which they regard as their best. We refer to those types of MGs as conventional. The identification of the best strategy is based on points

the agents allocate to each of their strategies in order to measure their performance. After each round of the game each agent evaluates the quality of each of his or her strategies, increasing the points of strategies which would have yielded a correct minority prediction. For a general overview of MG-type models we refer to [5].

The update rules of the MG look simple, but describe surprisingly complex cooperative processes. This is most visible in the non-trivial behaviour of the fluctuations of the total bid, the so-called market volatility [1, 6, 7, 2, 3]. The main control parameter in MGs is the ratio $\alpha = p/N$ of the number p of possible values for the public information over the number N of players. One observes a critical value α_c which marks a dynamical‡ phase transition, separating a non-ergodic phase ($\alpha < \alpha_c$) from an ergodic one ($\alpha > \alpha_c$). In the non-ergodic phase, the volatility is very sensitive to initial conditions [3, 8, 9], and the integrated response is infinite [4]. Moreover, in the stationary state the system exhibits persistent oscillations in the non-ergodic phase, whereas oscillations decay on finite time scales for $\alpha > \alpha_c$ [4, 10].

Analytical progress is possible using equilibrium and dynamical approaches and has resulted in analytical expressions for α_c , which are now regarded as exact [11, 4, 12, 13]. The generating functional analysis à la De Dominicis [14] has proven particularly valuable; it enabled a full understanding of the dynamics of the MG in the ergodic phase. In this formalism, the strategy selection dynamics of the agents is mapped onto a non-Markovian effective single agent process. In the case of conventional MGs, the microscopic laws and the resulting single-trader process are non-linear and resist analytical solution. Instead, one derives a coupled set of implicit equations for stationary states, from which one tries to extract the values of the persistent order parameters. In contrast to equilibrium systems, there are no fluctuation-dissipation relations which could be used to simplify those equations. In the ergodic phase the analysis can be simplified taking into account the existence of so-called ‘frozen agents’ (runaway solutions of the microscopic laws). A proper understanding of the dynamics in the non-ergodic regime, however, is still lacking. Moreover, for conventional MGs the market volatility (the MG’s main observable) cannot be expressed in terms of persistent order parameters. Instead, detailed knowledge of both the long-time and the short-time behaviour of the macroscopic order parameters is required. Hence, even in the ergodic phase, results for the volatility are so far restricted to approximations, whereas in the non-ergodic phase only approximate asymptotic results in the limit $\alpha \rightarrow 0$ are available [4]. For a recent review of dynamical MG analyses see e.g. [15]. Approximations for the volatility in the ergodic state are also accessible within the framework of replica theory [3].

In this paper we present a version of the MG which is analytically solvable, but nevertheless displays some of the interesting features found in the conventional MG. To this end we study the dynamics of a spherical version of the MG using the generating functional approach. Like in spherical p -spin glasses with polynomial equations of ‡ MGs do not obey detailed balance, so one can only speak about non-equilibrium phase transitions.

motion for the continuous microscopic degrees of freedom, *explicit* closed equations for the two-time correlation and response functions can be formulated [16].

A second control parameter, the radius r of the sphere to which the dynamics is confined, becomes relevant in the present model. Apart from the spherical constraint we choose the update rules to be linear in this paper, so that we can solve the resulting dynamical equations exactly, reminiscent of the $p = 2$ case known for spherical spin-glasses [17]. In particular we are able to compute the volatility in all regions of the phase diagram without making any approximations at any stage. In terms of the decision making of the individual agents the linear spherical model corresponds to allowing them to play linear combinations of strategies (rather than to pick the best one).

Despite its simple microscopic rules, the spherical MG as presented in this paper shows interesting behaviour and exhibits novel features as well as properties analogous to the ones of conventional MGs. In particular we find three distinct phases in the (α, r) -plane. Our analytical findings are verified convincingly by numerical simulations.

2. Model Definitions

Before defining the spherical version of the MG and giving an interpretation of its update rules, we will recall the dynamical rules of a conventional MG as studied for example in [4, 12]. We label the N agents in the MG with Roman indices. At each round t of the game each agent i takes a trading decision $b_i(t) \in \mathbb{R}$ (a ‘bid’) in response to the observation of public information $I_{\mu(t)}$ which is chosen randomly and independently from a set with $p = \alpha N$ possible values[§], so $\mu(t) \in \{1, \dots, \alpha N\}$. The rescaled total market bid at round t is defined as $A(t) = N^{-1/2} \sum_i b_i(t)$. Each agent i has $S \geq 2$ fixed trading strategies (look-up tables) $\mathbf{R}_{ia} = (R_{ia}^1, \dots, R_{ia}^{\alpha N})$ at his or her disposal, with $a = 1, \dots, S$. If agent i decides to use strategy a in round t of the game, his or her bid at this stage will be $b_i(t) = R_{ia}^{\mu(t)}$. All strategies \mathbf{R}_{ia} are chosen randomly and independently before the start of the game; they represent the quenched disorder of this problem. The behaviour of the MG was found not to depend much on the value of S [18, 19], nor on whether bids are discrete or continuous [2]. For convenience, we choose $S = 2$ and $\mathbf{R}_{ia} \in \{-1, 1\}^{\alpha N}$ in this paper. In order to decide which strategy to use, the agents assign points $p_{ia}(t)$ to each of their strategies, on the basis of what would have happened if they had played that particular strategy:

$$p_{ia}(t) = p_{ia}(t) - R_{ia}^{\mu(t)} A(t). \quad (1)$$

Strategies which would have produced a minority decision are thus rewarded. In the conventional MG, at each round t each player i uses the strategy in his or her arsenal with the highest score, i.e. $b_i(t) = R_{i\tilde{a}_i(t)}^{\mu(t)}$, where $\tilde{a}_i(t) = \arg \max_a p_{ia}(t)$. For $S = 2$ the rules (1) can then be simplified upon introducing the differences $q_i(t) = \frac{1}{2}[p_{i1}(t) - p_{i2}(t)]$. Thus, if $q_i(t) > 0$, agent i plays strategy \mathbf{R}_{i1} , whereas for $q_i(t) < 0$ he or she plays \mathbf{R}_{i2} .

[§] This is the so-called MG with random external information; in the early MG definition [18] the external information was not random but coded for the actual history of the global market.

Hence, in the conventional MG $b_i(t) = \omega_i^{\mu(t)} + \text{sgn}[q_i(t)]\xi_i^{\mu(t)}$, where $\omega_i = \frac{1}{2}[\mathbf{R}_{i1} + \mathbf{R}_{i2}]$ and $\xi_i = \frac{1}{2}[\mathbf{R}_{i1} - \mathbf{R}_{i2}]$. The evolution of the $\{q_i\}$ is given by

$$q_i(t+1) = q_i(t) - \xi_i^{\mu(t)} \left[\Omega^{\mu(t)} + \frac{1}{\sqrt{N}} \sum_j \xi_j^{\mu(t)} \text{sgn}[q_j(t)] \right] \quad (2)$$

with $\Omega = N^{-1/2} \sum_j \omega_j$. Equation (2) defines the standard (or so-called ‘on-line’) MG. Alternatively, corresponding to updating the $\{q_i\}$ only every $\mathcal{O}(N)$ time-steps, one might define the dynamics in terms of an average over all possible values of the external information in (2), resulting in the so-called (conventional) ‘batch’ MG [4]:

$$q_i(t+1) = q_i(t) - h_i - \sum_j J_{ij} \text{sgn}[q_j(t)]. \quad (3)$$

Here $J_{ij} = 2N^{-1}\xi_i \cdot \xi_j$ and $h_i = 2N^{-1/2}\xi_i \cdot \Omega$. See [13] for stochastic extensions and [10] for consideration of the effects of anti-correlation of strategies on the comparison of on-line and batch models.

The batch model (3) is particularly suitable for being replaced by a spherical version. We first linearize (3), and subsequently normalize^{||} the vector (q_1, \dots, q_N) to a fixed length $r > 0$ at each iteration step t , resulting in the spherical batch MG:

$$[1 + \lambda(t+1)]q_i(t+1) = q_i(t) - h_i - \sum_j J_{ij} q_j(t), \quad (4)$$

$$\frac{1}{N} \sum_i q_i^2(t) = r^2 \quad \text{for all } t. \quad (5)$$

The values of the constraining forces $\lambda(t)$ in (4) follow from (5); we exclude artificial sign changes by insisting on $1 + \lambda(t) > 0$ for all t . We note that our model (4,5) has no analogue of the *tabula rasa* MG initialization, $q_i(0) = 0$ for all i , often employed in the conventional MG. We also note that the $\{q_i\}$ of the conventional MG (3) do not satisfy a spherical constraint, unlike the spins of a conventional Ising spin system. There is thus no reason for restricting oneself to $r = 1$. In fact, r is a new control parameter and the system exhibits phase behaviour in the (α, r) -plane with interesting differences from the conventional game.

The linearity of (4) implies that agents now play *linear combinations* of their strategies. Upon presentation of public information I_μ at time t the bid of player i in a corresponding on-line game is

$$b_i(t) = \frac{1}{2}[1 + q_i(t)]R_{i1}^\mu + \frac{1}{2}[1 - q_i(t)]R_{i2}^\mu. \quad (6)$$

The main object of natural interest in MGs is the volatility, which describes the standard deviation of the total (re-scaled) market bid

$$A^\mu[\mathbf{q}(t)] = \frac{1}{\sqrt{N}} \sum_i [\omega_i^\mu + q_i(t)\xi_i^\mu]. \quad (7)$$

^{||} The spherical normalisation is necessary to suppress possible runaway solutions corresponding to eigenmodes of the linear update rule with eigenvalues of a modulus larger than one.

In the on-line models the relevant averages are over the stochasticity of the ‘information’. In deterministic batch problems, such as discussed here, these averages are replaced by ones over μ : $\langle A_t \rangle = p^{-1} \sum_{\mu=1}^p A^\mu[\mathbf{q}(t)]$ and $\langle A_t A_{t'} \rangle = p^{-1} \sum_{\mu=1}^p A^\mu[\mathbf{q}(t)] A^\mu[\mathbf{q}(t')]$. The volatility is defined as $\sigma_t^2 = \langle A_t^2 \rangle - \langle A_t \rangle^2$. Here we follow [4] and define a more general object, the volatility matrix $\Xi_{tt'} = \langle A_t A_{t'} \rangle - \langle A_t \rangle \langle A_{t'} \rangle$:

$$\Xi_{tt'} = \frac{1}{p} \sum_{\mu=1}^p A^\mu[\mathbf{q}(t)] A^\mu[\mathbf{q}(t')] - \left[\frac{1}{p} \sum_{\mu=1}^p A^\mu[\mathbf{q}(t)] \right] \left[\frac{1}{p} \sum_{\mu=1}^p A^\mu[\mathbf{q}(t')] \right]. \quad (8)$$

Note that $\sigma_t^2 = \Xi_{tt}$. Random trading, with $\mathbf{q}(t)$ taken randomly and independently from the sphere $\mathbf{q}^2(t) = Nr^2$ at each time t , would result in $\langle A_t \rangle = \mathcal{O}(N^{-\frac{1}{2}})$ and $\Xi_{tt'} = \frac{1}{2} + \frac{1}{2}r^2\delta_{tt'} + \mathcal{O}(N^{-\frac{1}{2}})$. The volatility measures the efficiency of the market, with $\sigma_t^2 = 0$ corresponding to a perfect match between supply and demand at time t .

3. Macroscopic Dynamics

The similarity between the spherical batch MG (4,5) and the conventional batch MG (3) allows us to obtain the effective single trader equations for (4,5) simply by making the substitutions $q(t+1) \rightarrow [1 + \lambda(t+1)]q(t+1)$ and $\text{sgn}[q(t)] \rightarrow q(t)$ in the results of [4] (found within the generating functional analysis framework, in the limit $N \rightarrow \infty$):

$$[1 + \lambda(t+1)]q(t+1) = q(t) + \theta(t) - \alpha \sum_{t'} (\mathbf{I} + G)_{tt'}^{-1} q(t') + \sqrt{\alpha} \eta(t). \quad (9)$$

Here $\theta(t)$ is an external perturbation field introduced to generate response functions and $\eta(t)$ is a zero-average Gaussian noise, characterized by the following covariance matrix (with $D_{tt'} = 1 + C_{tt'}$ and $\mathbf{I}_{tt'} = \delta_{tt'}$):

$$\Sigma_{tt'} = \langle \eta(t) \eta(t') \rangle_* = [(\mathbf{I} + G)^{-1} D (\mathbf{I} + G^T)^{-1}]_{tt'}. \quad (10)$$

The matrices C and G and the constraining forces $\lambda(t)$ are the dynamical order parameters of the problem, to be determined self-consistently by solving

$$C_{tt'} = \langle q(t) q(t') \rangle_*, \quad G_{tt'} = \frac{\partial}{\partial \theta(t')} \langle q(t) \rangle_*, \quad C_{tt} = r^2. \quad (11)$$

One always has $\langle q(t) \rangle_* = 0$. The physical meaning of C and G is given by

$$C_{tt'} = \lim_{N \rightarrow \infty} \frac{1}{N} \sum_i \overline{\langle q_i(t) q_i(t') \rangle}, \quad (12)$$

$$G_{tt'} = \lim_{N \rightarrow \infty} \frac{1}{N} \sum_i \frac{\partial}{\partial \theta_i(t')} \overline{\langle q_i(t) \rangle}, \quad (13)$$

where $\overline{\dots}$ denotes an average over the disorder, i.e. over the space of all strategies in the context of the MG. The brackets $\langle \dots \rangle_*$ in (10) and (11) refer to averaging over the realisations of the process (9), i.e. over the noise $\{\eta(t)\}$. As usual, the single-agent process (9) is non-Markovian.

It is possible to convert the system (9,10,11) into a pair of explicit iterative equations for C and G . An explicit equation for C results upon multiplying (9)

by $q(t')$ and subsequently averaging over the noise. We make use of the identity $\langle \eta(t)q(t') \rangle_* = \sqrt{\alpha} \sum_s (\Sigma_{ts} G_{t's})$ (derived via an integration by parts in the generating functional; see [4] for an analogous identity in the conventional MG). To deal with G (which obeys causality: $G_{tt'} = 0$ for $t \leq t'$) one takes a field derivative of (9), followed by averaging. The result reads:

$$[1 + \lambda(t+1)] C_{t+1,t'} = C_{tt'} + \alpha [(\mathbf{I} + G)^{-1} D (\mathbf{I} + G^T)^{-1} G^T]_{tt'} - \alpha [(\mathbf{I} + G)^{-1} C]_{tt'}, \quad (14)$$

$$[1 + \lambda(t+1)] G_{t+1,t'} = G_{tt'} - \alpha [(\mathbf{I} + G)^{-1} G]_{tt'} + \delta_{tt'}. \quad (15)$$

These coupled equations have to be solved subject to the constraint $C_{tt} = r^2$ for all $t \geq 0$. Furthermore, as in [4] one finds for $N \rightarrow \infty$ that the rescaled disorder-averaged average bid $\overline{\langle A_t \rangle}$ is zero at any time, and that the disorder-averaged volatility matrix (8) is proportional to the covariance matrix of the single-trader noise:

$$\lim_{N \rightarrow \infty} \overline{\Xi}_{tt'} = \frac{1}{2} \Sigma_{tt'} = \frac{1}{2} [(\mathbf{I} + G)^{-1} D (\mathbf{I} + G^T)^{-1}]_{tt'}. \quad (16)$$

The dynamic order parameters in the spherical model are prescribed in full by (14,15), with the constraints $C_{tt} = r^2$ and $1 + \lambda(t) > 0$. As in [4], they can be calculated iteratively, starting from $(t, t') = (0, 0)$, and upon using causality (i.e. $[G^n]_{tt'} = 0$ for $n > t - t'$). Given the prescribed values $C_{00} = r^2$ and $G_{00} = 0$ one finds, for instance:

$$\lambda(1) = -1 + (1 + \alpha(r^{-2} - 1) + \alpha^2)^{1/2}, \quad (17)$$

$$G_{10} = [1 + \alpha(r^{-2} - 1) + \alpha^2]^{-\frac{1}{2}}, \quad (18)$$

$$C_{10} = \frac{r^2(1 - \alpha)}{\sqrt{1 + \alpha(r^{-2} - 1) + \alpha^2}} \quad (19)$$

(note: $G_{11} = 0$ and $C_{11} = r^2$). From these follow the volatility matrix elements:

$$\Sigma_{00} = 1 + r^2, \quad (20)$$

$$\Sigma_{10} = 1 - \frac{\alpha r^2 + 1}{\sqrt{1 + \alpha(r^{-2} - 1) + \alpha^2}}, \quad (21)$$

$$\Sigma_{11} = 1 + r^2 - \frac{2}{\sqrt{1 + \alpha(r^{-2} - 1) + \alpha^2}} + \frac{1 - r^2(1 - 2\alpha)}{1 + \alpha(r^{-2} - 1) + \alpha^2}. \quad (22)$$

This iteration can be carried out for an arbitrary number of time steps; in practice, however, the terms become prohibitively more complicated for increasing times. Alternatively, one may iterate (14,15) numerically. Unlike the procedure proposed in [20] to generate realisations of the single trader process, the iteration of (14,15) does not require averaging over the single agent noise, and thus provides very precise data (albeit that numerically inverting the $t \times t$ matrices in (14,15) becomes more and more costly as the number of time steps increases).

One observes that, due to the explicit form of (14,15) (and in sharp contrast to the similar calculation in [4]), the temporal evolution of the macroscopic order parameters is completely *independent of initial conditions*: as long as the constraint

$\lim_{N \rightarrow \infty} N^{-1} \sum_{i=1}^N q_i(0)^2 = C_{00} = r^2$ is met the distribution $P(q_i(0))$ from which the initial point differences are drawn is irrelevant for the values of both C and G at finite times as well as for the macroscopic stationary state. We have verified this in numerical simulations, initializing the dynamics with different distributions for the $q_i(0)$, but all with second moment $N^{-1} \sum_{i=1}^N q_i^2(0) = r^2$. This property of the spherical MG is quite distinct from the conventional MG, where the explicit analysis of the first few time steps as presented in [4] reveals that the values of the correlation and response functions at finite times depend on the higher moments of $P(q_i(0))$ as well, and not only on its variance. As far as the stationary state of the conventional MG is concerned the interest so far has mainly focussed on starts of the form $|q_i(0)| = q_0$ for all i , with $q_0 = 0$ for *tabula rasa* starts and $q_0 > 0$ for biased starts. Crucial differences between the two cases have been found in the non-ergodic regime [3, 8, 9]. We have extended this analysis and have performed simulations of the conventional batch game with different initial distributions for the $q_i(0)$ all with the same second moment q_0^2 . For fixed second moment we find that *qualitatively* the stationary volatility does not depend on the higher moments of $P(q_i(0))$, but that differences in the *quantitative* values are found for different shapes of the initial distribution of point differences.

Let us finally inspect the solution of (14,15) for small α and finite times. By induction one finds

$$\lambda(t) = \mathcal{O}(\alpha), \quad G_{tt'} = \Theta_{tt'} + \mathcal{O}(\alpha), \quad C_{tt'} = r^2 + \mathcal{O}(\alpha),$$

where $\Theta_{tt'} = 1$ if $t > t'$ and $\Theta_{tt'} = 0$ otherwise. For the volatility we find $\Sigma_{tt} = \mathcal{O}(\alpha^2)$ for all finite $t \geq 2$. We conclude that for small α the system is in a completely frozen state, with a divergent integrated response and vanishing volatility.

4. Analysis of Stationary States

4.1. Implications of Time-Translation Invariance

We now focus on time-translation invariant solutions of the dynamical equations (14,15), i.e. we consider the system long after any initial equilibration and study solutions of the form

$$C_{tt'} = C(t - t'), \quad G_{tt'} = G(t - t'), \quad \lambda(t) = \lambda. \quad (23)$$

Then all matrices in (14,15) become Toeplitz matrices, and hence they commute. Given (23) it is natural to express the dynamics in terms of the Fourier transforms of the correlation and response functions. We use the following notation:

$$C(\tau) = \int_{-\pi}^{\pi} \frac{d\omega}{2\pi} e^{i\omega\tau} \tilde{C}(\omega), \quad \tilde{C}(\omega) = \sum_{\tau} e^{-i\omega\tau} C(\tau) \quad (24)$$

and similarly for G . The equations (14,15) subsequently translate into

$$\tilde{\Delta}(\omega) \tilde{C}(\omega) = \frac{\alpha \tilde{D}(\omega) \tilde{G}(\omega)^*}{|1 + \tilde{G}(\omega)|^2} - \frac{\alpha \tilde{C}(\omega)}{1 + \tilde{G}(\omega)}, \quad (25)$$

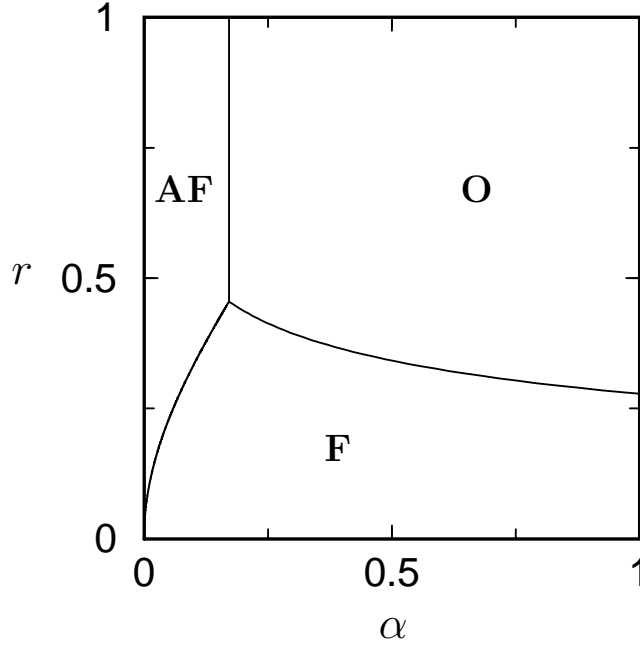


Figure 1. Phase diagram of the spherical MG, displaying three phases: **O**, oscillating correlation function and finite integrated response; **F**, frozen phase with finite integrated response; and **AF**, anomalous frozen phase with diverging integrated response. Throughout the phase AF the volatility is zero. The O→F transition is defined by (39), and the F→AF transition is defined by (46); both are continuous. The discontinuous transition from O→AF occurs at $\alpha = 3 - 2\sqrt{2} \approx 0.172$. The triple point corresponds to $\alpha = 3 - 2\sqrt{2}$ and $r = r^* \approx 0.455$.

$$\tilde{\Delta}(\omega)\tilde{G}(\omega) = 1 - \frac{\alpha\tilde{G}(\omega)}{1 + \tilde{G}(\omega)}, \quad (26)$$

where $\tilde{\Delta}(\omega) = (1 + \lambda)e^{i\omega} - 1$, and $\tilde{G}(\omega)^*$ denotes the complex conjugate of $\tilde{G}(\omega)$. Since $\tilde{D}(\omega) = \tilde{C}(\omega) + 2\pi\delta(\omega)$, and upon defining the integrated static response $\chi = \sum_{\tau} G(\tau) = \tilde{G}(0)$, we may rewrite (25) as

$$\left[\tilde{\Delta}(\omega)|1 + \tilde{G}(\omega)|^2 + \alpha \right] \tilde{C}(\omega) = 2\pi\alpha\chi\delta(\omega). \quad (27)$$

Note that considering the case $\omega = 0$ in (26) allows us to express λ in terms of χ :

$$\lambda = \frac{1 + \chi(1 - \alpha)}{\chi(1 + \chi)}. \quad (28)$$

Finally, in the stationary state the volatility matrix $\bar{\Xi}$ is also of the Toeplitz form $\bar{\Xi}_{tt'} = \bar{\Xi}(t - t')$ and thus the volatility $\sigma^2 = \bar{\Xi}(0)$ can be expressed as

$$\sigma^2 = \frac{1}{2} \int_{-\pi}^{\pi} \frac{d\omega}{2\pi} \frac{\tilde{C}(\omega)}{|1 + \tilde{G}(\omega)|^2} + \frac{1}{2(1 + \chi)^2}. \quad (29)$$

Since initial conditions play no role in the macroscopic dynamics, we must conclude that as soon as multiple stationary solutions exist only one of these will ever be realized.

Before we give a detailed account of the further analysis of the dynamical equations, we briefly summarise our results. We find that, depending on the control parameters α and r , the system displays three distinct phases, as illustrated in figure 1:

- (i) a phase with finite integrated response and oscillatory behaviour of the correlation function (O),
- (ii) a frozen phase with finite integrated response (F),
- (iii) a frozen phase exhibiting anomalous integrated response which grows linearly with time (AF).

We will now proceed to obtain exact solutions of the dynamical equations in each of the three phases.

4.2. Stationary States without Anomalous Response

We first inspect stationary states with finite χ , i.e. those for which perturbations will decay sufficiently fast. It now follows from (27) that, for any $\omega \neq 0$, $\tilde{C}(\omega)$ can be non-zero only if $\tilde{\Delta}(\omega)|1 + \tilde{G}(\omega)|^2 + \alpha = 0$. This requires $\tilde{\Delta}(\omega)$ to be real, which is possible only for $\omega = 0, \pi$. We conclude that $\tilde{C}(\omega) = 2\pi c_0\delta(\omega) + 2\pi c_1\delta(\omega - \pi)$, or equivalently

$$C(\tau) = c_0 + c_1(-1)^\tau. \quad (30)$$

Here c_0 and c_1 (which will depend on the parameters α and r , as will χ) are coupled via the spherical constraint: $c_0 + c_1 = r^2$. Insertion of (30) into (27) leads to the following two coupled equations

$$c_0 [\alpha + \lambda(1 + \chi)^2] = \alpha\chi, \quad (r^2 - c_0) [\alpha - (\lambda + 2)(1 + \chi')^2] = 0 \quad (31)$$

with $\chi' = \sum_t (-1)^t G(t) = \tilde{G}(\pi)$ measuring the response to persistent oscillating perturbations. These equations are to be solved in combination with (26). We conclude that there are two types of stationary states with finite χ : a frozen state, where $c_0 = r^2$ (so $c_1 = 0$), and an oscillating state, where $c_0 < r$. We will work out their properties separately below. For solutions of the form (30) we can also work out (29) further:

$$\sigma^2 = \frac{1 + c_0}{2(1 + \chi)^2} + \frac{(r^2 - c_0)}{2(1 + \chi')^2}. \quad (32)$$

Oscillating stationary states without anomalous response. Here $c_0 < r^2$, and the remaining four (coupled but closed) equations to be solved to find the stationary state include one expression for χ' which one obtains by choosing $\omega = \pi$ in (26):

$$c_0 = \frac{\alpha\chi}{\alpha + \lambda(1 + \chi)^2}, \quad \alpha = (\lambda + 2)(1 + \chi')^2, \quad (33)$$

$$\lambda = \frac{1 + \chi(1 - \alpha)}{\chi(1 + \chi)}, \quad \lambda + 2 = -\frac{1 + \chi'(1 - \alpha)}{\chi'(1 + \chi')}. \quad (34)$$

The set (33,34) allows for two types of solutions. The first, where $\lambda = \alpha - 1 + 2\sqrt{\alpha}$, obeys the requirement $1 + \lambda > 0$ for all α . One must in fact demand $\lambda > 0$ in order to

have a finite χ (as required), and we reject $\chi < 0$ solutions on physical grounds. This leaves:

$$\lambda = \alpha - 1 + 2\sqrt{\alpha}, \quad (35)$$

$$\chi = \frac{1 - \alpha - \sqrt{\alpha} + \sqrt{2\alpha^{3/2} + \alpha^2}}{-1 + 2\sqrt{\alpha} + \alpha}, \quad (36)$$

$$\chi' = -\frac{1}{1 + \sqrt{\alpha}}. \quad (37)$$

We note that λ , χ , χ' and c_0 are independent of r ; only c_1 depends on r via $c_1 = r^2 - c_0$. The second type of solution, where $\lambda = \alpha - 1 - 2\sqrt{\alpha}$, meets our requirement $\lambda + 1 > 0$ only for $\alpha > 4$. It turns out that such solutions are never realized, so we will not give their equations in full. We have now determined all order parameters and the volatility in explicit form: c_0 follows from insertion of (35,36) into the first equation of (33), whereas the volatility follows upon inserting c_0 and (36,37) into (32). For $\alpha \rightarrow \infty$ one finds $\lim_{\alpha \rightarrow \infty} \chi = 0$, $\lim_{\alpha \rightarrow \infty} \lambda/\alpha = 1$, so that $\lim_{\alpha \rightarrow \infty} c_0 = 0$; the amplitude of the oscillations in the correlations increases with increasing α .

The present solution breaks down when either $\chi \rightarrow \infty$ or $c_1 \rightarrow 0$. The corresponding mathematical conditions are found to be $\alpha = \alpha_{c,1}$ (with $\chi < \infty$ for $\alpha > \alpha_{c,1}$) and $\alpha = \alpha_{c,2}(r)$ (with $c_1 > 0$ for $\alpha > \alpha_{c,2}(r)$), respectively, where

$$\alpha_{c,1} = 3 - 2\sqrt{2} \approx 0.172, \quad (38)$$

$$\alpha_{c,2}(r) = \left[1 - \frac{2 + 1/r^2}{2\sqrt{1 + 1/r^2}} \right]^2. \quad (39)$$

We note that $\alpha_{c,1} = \alpha_{c,2}(r)$ at $r = r^* = \sqrt{\alpha_{c,1}/(1 - \alpha_{c,1})} \approx 0.455$, and that $\alpha_{c,2}(r) > \alpha_{c,1}$ for $r < r^*$ and $\alpha_{c,2}(r) < \alpha_{c,1}$ for $r > r^*$. Thus one expects that, as α is lowered for any $r > r^*$, the amplitude of the oscillations of the correlations remains positive until the critical value $\alpha_{c,1}$ is reached and a transition to a state with anomalous response occurs. At this point one has

$$\lim_{\alpha \downarrow \alpha_{c,1}} \sigma^2 = \frac{1}{3 - 2\sqrt{2}} \left(r^2 - \frac{3 - 2\sqrt{2}}{2(\sqrt{2} - 1)} \right). \quad (40)$$

For $r < r^*$ the oscillatory behaviour of the correlations breaks down as α is lowered before anomalous response sets in, and the system enters a frozen state with finite integrated response.

Frozen stationary states without anomalous response. Here $c_0 = r^2$, and there is no need to calculate χ' ; the coupled equations to be solved are simply

$$\lambda\chi^2 + (2\lambda - \alpha/r^2)\chi + \lambda + \alpha = 0, \quad (41)$$

$$\lambda\chi^2 + (\alpha - 1 + \lambda)\chi - 1 = 0, \quad (42)$$

from which we can determine λ and χ to be:

$$\lambda = -1 - \alpha + \frac{(2 + 1/r^2)\sqrt{\alpha}}{\sqrt{1 + 1/r^2}}, \quad (43)$$

$$\chi = [\sqrt{\alpha}\sqrt{1 + 1/r^2} - 1]^{-1}. \quad (44)$$

Upon inserting (44) and the relation $c_0 = r^2$, one finds that our exact expression (32) for the volatility simplifies to

$$\sigma^2 = \frac{1}{2} \left[\sqrt{r^2 + 1} - r/\sqrt{\alpha} \right]^2. \quad (45)$$

The present frozen state will cease to be a consistent solution at the point where χ diverges. Equation (44) states that this happens at $\alpha = \alpha_{c,3}(r)$, where

$$\alpha_{c,3}(r) = r^2/(r^2 + 1). \quad (46)$$

The line $\alpha = \alpha_{c,3}(r)$ marks the transition between a frozen state with finite integrated response (for $\alpha > \alpha_{c,3}(r)$), and an anomalous frozen state (for $\alpha < \alpha_{c,3}(r)$). According to (45) it also coincides with the line where the volatility vanishes.

4.3. Frozen States with Anomalous Response

Numerical simulations for small α and large r reveal a parameter regime with a stationary state in which the volatility vanishes, $\sigma^2 = 0$, and where all agents are frozen in such a way that

$$C(\tau) = r^2, \quad \lambda(\tau) = 0, \quad \chi = \infty. \quad (47)$$

These three identities clearly hold at the transition line (46), where anomalous response first emerges in the frozen state. In this subsection we demonstrate that our dynamical equations (14,15) indeed allow for self-consistent stationary state solutions with the properties (47). Note that (47) directly imply that $\sum_{\tau} [\mathbf{I} + G]^{-1}(\tau) = (1 + \chi)^{-1} = 0$, and hence also $\sigma^2 = 0$. Insertion of (47) as *ansätze* into (14,15) now gives:

$$0 = [(\mathbf{I} + G)^{-1}D(\mathbf{I} + G^T)^{-1}G^T](\tau) - [(\mathbf{I} + G)^{-1}C](\tau), \quad (48)$$

$$G(\tau + 1) = G(\tau) + \alpha(\mathbf{I} + G)^{-1}(\tau) + (1 - \alpha)\delta(\tau), \quad (49)$$

where $\delta(\tau) = 1$ if $\tau = 0$ and $\delta(\tau) = 0$ otherwise. We define the persistent response $g = \lim_{T \rightarrow \infty} T^{-1} \sum_{\tau \leq T} G(\tau)$, and sum both sides of (49) from $\tau = 0$ to $\tau = \ell$, to get:

$$G(\ell + 1) = 1 - \alpha + \alpha \sum_{\tau \leq \ell} (\mathbf{I} + G)^{-1}(\tau). \quad (50)$$

We conclude that $g = 1 - \alpha$. From this, in turn, one infers for $\alpha < 1$ that indeed $\chi = \sum_{\tau} G(\tau) = \infty$, which confirms in retrospect that our *ansätze* (47) indeed solve our dynamical laws (48,49).

5. The Phase Diagram and its Verification

In the previous section we have identified three distinct phases, which according to the extensive numerical simulations described below exhaust the phase diagram in the (α, r) -plane of the present spherical MG. We have also derived explicit expressions for the macroscopic order parameters and the volatility in all three phases, and we have

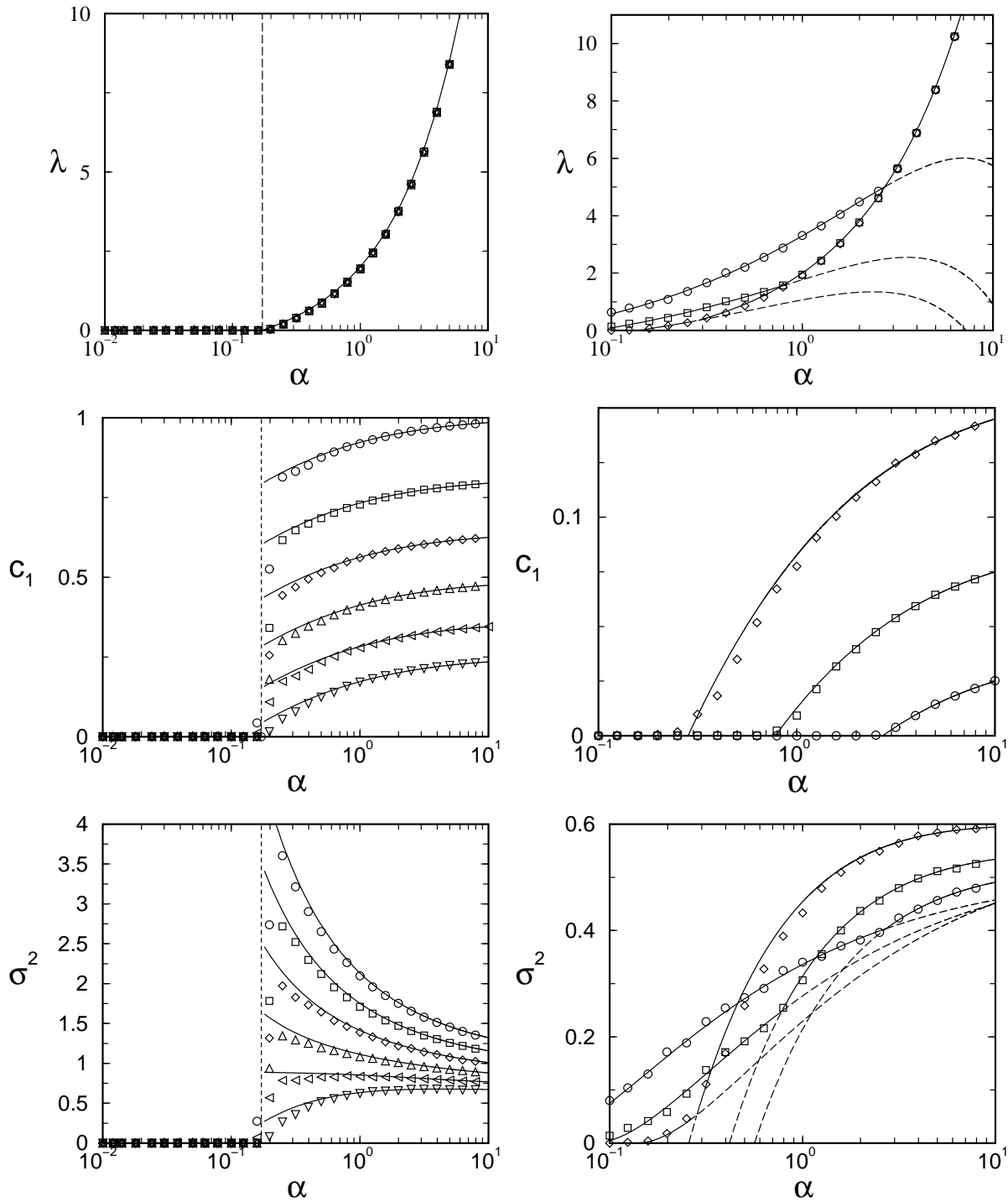


Figure 2. Verification of O→AF and O→F transitions. Left pictures: Lagrange parameter λ , oscillation amplitude c_1 and volatility σ^2 versus α , for $r = 1.0, 0.9, 0.8, 0.7, 0.6, 0.5$ (from top to bottom in the panels showing c_1 and σ^2). Here we expect to see the O→AF transition. Markers: simulations; solid lines: theory. The dashed vertical line marks the predicted location $\alpha_{c,1}$ of the O→AF transition. Right pictures: the same observables shown versus α , but now for $r = 0.4, 0.3, 0.2$; here we expect to see the O→F transition. Markers: simulations for $r = 0.2$ (circles), $r = 0.3$ (squares) and $r = 0.4$ (diamonds); solid lines: theory. The lines are continued as dashed lines into the opposite phases, where they should no longer be valid.

been able to calculate the various phase boundaries in explicit form. Our results may be summarised as follows:

$$\begin{aligned}
\alpha > \max\{\alpha_{c,1}, \alpha_{c,2}(r)\} &: && \text{oscillating phase (O)} \\
&&& \text{oscillating } C(t), \text{ finite } \chi \\
r < r^*, \alpha_{c,3}(r) < \alpha < \alpha_{c,2}(r) &: && \text{frozen phase (F)} \\
&&& \text{constant } C(t), \text{ finite } \chi \\
\alpha < \min\{\alpha_{c,1}, \alpha_{c,3}(r)\} &: && \text{anomalous frozen phase (AF)} \\
&&& \text{constant } C(t), \text{ infinite } \chi
\end{aligned}$$

with

$$\alpha_{c,1} = 3 - 2\sqrt{2}, \quad \alpha_{c,2}(r) = \left[1 - \frac{r + 1/2r}{\sqrt{r^2 + 1}}\right]^2, \quad \alpha_{c,3}(r) = \frac{r^2}{r^2 + 1}. \quad (51)$$

The resulting phase diagram is shown in figure 1. Let us briefly discuss its main features. For $r > r^*$ the behaviour of the spherical MG is similar to that of its conventional counterparts, with a divergence of χ at some fixed critical α and χ remaining infinite as α is reduced further to zero. There are crucial differences though: Firstly, in the conventional MG persistent oscillations are found only for $\alpha < \alpha_c$, while they decay above the transition. The opposite is the case in the spherical model. Secondly, in the conventional MG the volatility σ^2 is a smooth function of α across the transition. In the spherical model we find that the volatility (and the amplitude c_1 of the oscillations as well) exhibits a jump at $\alpha = \alpha_{c,1}$ for $r > r^*$. The discontinuity of σ^2 follows immediately from the nonzero value of (40) for $r > r^*$, which gives σ^2 in the phase O close to the O→AF transition, whereas one has $\sigma^2 = 0$ throughout the AF phase. The magnitude of the jump decreases as r is lowered and finally vanishes at $r = r^*$. Below $r = r^*$ no discontinuities are present and one finds an intermediate regime, where the system freezes, but as yet with a finite χ . Only as α is lowered further a transition to a frozen phase with anomalous integrated response takes place at $\alpha = \alpha_{c,3}(r)$, and below $\alpha_{c,3}(r)$ both the volatility and the normalisation factor λ vanish identically.

We have tested our theoretical predictions against numerical simulations of the spherical MG. The data shown in the figures are all obtained from simulations of the batch process (4,5) with $N = 500$ players, and averaged over 20 realisations of the disorder (i.e. the realisations of the strategies). All measurements are temporal averages over 250 time steps, preceded by 250 ‘equilibration’ steps. We focus on the parameter regions where the various phase transitions are predicted to occur and depict the values of the stationary order parameters λ and c_1 as well as the volatility σ^2 as indicators for the predicted transitions. The precise locations of the various transitions are given in (51).

Figure 2 concerns the O→AF and O→F transitions. For $r > r^* \approx 0.455$ we expect to see the O→AF transition. Here our theory predicts that $\lambda = \alpha - 1 + 2\sqrt{\alpha}$ for $\alpha > \alpha_{c,1}$, and $\lambda = 0$ for $\alpha < \alpha_{c,1}$. At $\alpha_{c,1}$ the volatility and the oscillation amplitude c_1 should both jump discontinuously to zero. For $r < r^*$, on the other hand we should observe the O→F transition where c_1 goes to zero continuously at $\alpha = \alpha_{c,2}(r)$. We

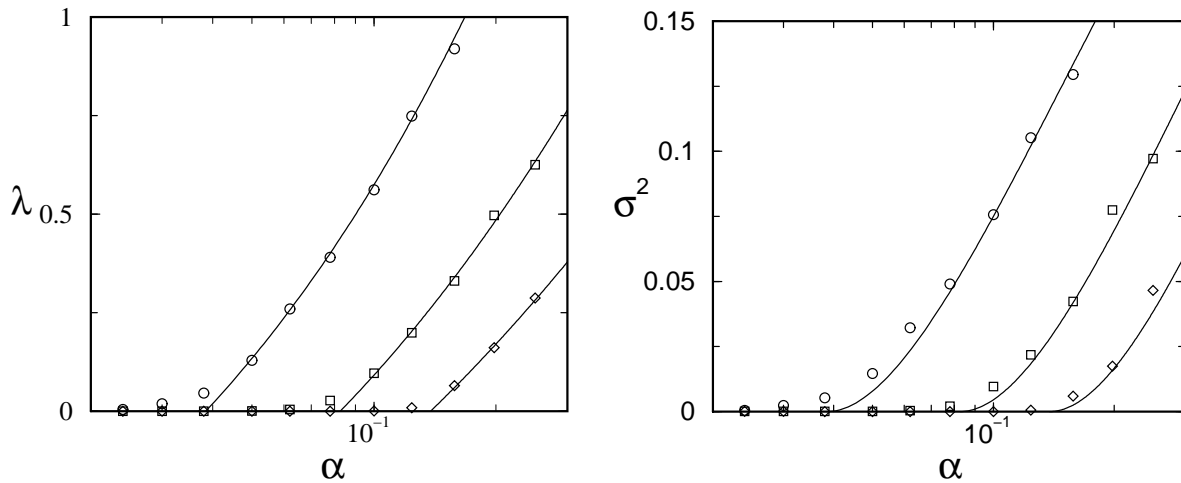


Figure 3. Verification of F→AF transition. Lagrange parameter λ (left) and volatility σ^2 (right) versus α , for $r = 0.2$ (circles), $r = 0.3$ (squares) and $r = 0.4$ (diamonds). Solid lines: theory. Both observables are predicted to converge to zero as the transition $\alpha = \alpha_{c,3}(r)$ is approached from above, and to remain zero below the transition.

also expect λ and σ^2 to be continuous at this transition, albeit their derivatives with respect to α change discontinuously. The data in figure 2 reveal full agreement between theory and simulation (up to finite size effects close to the transitions). Although we restrict ourselves to $r \leq 1$ in figure 2, we have verified that the qualitative behaviour of the system remains unchanged for larger values of r and that the very good agreement between theory and simulation continues to hold for $r > 1$. Figure 3 concerns the F→AF transition, where λ and σ^2 are predicted to vanish as α approaches $\alpha_{c,3}(r)$ from above. Again we find good agreement between theory and numerical experiment.

6. Conclusions

In this paper we have introduced a spherical version of the batch minority game, with random public information. In this model the non-linear update rule of the conventional game is replaced by an iteration prescription which is linear in the microscopic degrees of freedom (the point differences $q_i(t)$), complemented by a spherical constraint $N^{-1} \sum_i q_i^2(t) = r^2$. The spherical MG is designed to be exactly solvable in the thermodynamic limit. In terms of the decision making of the individual agents, the linearised microscopic dynamical laws corresponds to allowing the agents to play linear combinations of their two strategies. The relevant control parameters of the spherical MG are the radius r of the sphere to which the dynamics is confined and the ratio $\alpha = p/N$ of the number of possible values of the external information over the number of agents.

Using the dynamic mean field theory introduced by De Dominicis we are able to perform the average over the disorder and to take the thermodynamic limit. This formalism reduces the original N -agent dynamics to a non-Markovian effective single-

agent stochastic process. Like in spherical spin-glass models, the temporal evolution of the macroscopic order parameters (the correlation and response functions) can be formulated in terms of a pair of coupled iterative equations, without referring to the microscopic single effective-agent process. Assuming the existence of a time-translation invariant stationary state we are able to solve these equations exactly, and to compute the order parameters in the stationary state as well as the stationary volatility at every point of the phase diagram without making any approximations.

We find that, although the update rule is relatively simple compared to the conventional MG, the spherical MG displays a remarkably rich structure. Depending on r and α the system exhibits three distinct phases, two without anomalous response (an oscillating and a frozen state) and a further frozen phase with diverging integrated response. As described above the spherical model exhibits some similarities as well as intriguing differences compared to conventional MGs. The four main differences are (i) the absence of any macroscopic dynamical effect of the choice of the initial microscopic state in the spherical game, (ii) the fact that, for any r , the volatility is always zero close to $\alpha = 0$ whereas in the conventional MGs both high-volatility and low-volatility solutions can be found, (iii) persistent oscillations in the spherical MG, which increase for increasing α and vanish for low α , where in the conventional batch MG persistent oscillations can only be found in the low- α regime and (iv) the discontinuous dependence of the volatility on α in the spherical MG for $r > r^*$.

In summary, our study demonstrates that the dynamical rules of the conventional MG can be simplified to obtain a completely solvable spherical version, which still displays a non-trivial phase diagram and some novel features, which are not observed in conventional MGs. It would be interesting to study further the mathematical properties of the spherical model, such as the relaxation towards the stationary state and possible ageing phenomena.

Acknowledgements

The authors would like to thank EPSRC for financial support under research grant GR/M04426 and studentship 00309273. T.G. acknowledges the award of a Rhodes Scholarship and support by Balliol College, Oxford. Fruitful discussions with J.P. Garrahan are gratefully acknowledged.

References

- [1] Challet D and Zhang Y-C 1997 *Physica A* **246** 407
- [2] Cavagna A, Garrahan J P, Giardinà I, and Sherrington D 1999 *Phys. Rev. Lett.* **83** 4429
- [3] Challet D, Marsili M and Zecchina R 2000 *Phys. Rev. Lett.* **84** 1824
- [4] Heimel J A F and Coolen A C C 2001 *Phys. Rev. E* **63** 056121
- [5] Challet D, <http://www.unifr.ch/econophysics/minority>
- [6] Cavagna A 1999 *Phys. Rev. E* **59** R3783
- [7] Savit R, Manuca R and Riolo R 1999 *Phys. Rev. Lett.* **82** 2203
- [8] Marsili M, Challet D and Zecchina R 2000 *Physica A* **280** 522

- [9] Garrahan J P, Moro E and Sherrington D 2000 *Phys. Rev E* **62** R9
- [10] Sherrington D and Galla T 2003 *Physica A* (in press), preprint [cond-mat/0301328](#)
- [11] Challet D, Marsili M and Zhang Y-C 2000 *Physica A* **276** 284
- [12] Coolen A C C and Heibel J A F 2001 *J. Phys. A: Math. Gen.* **34** 10783
- [13] Coolen A C C, Heibel J A F and Sherrington D 2001 *Phys. Rev. E* **65** 016126
- [14] De Dominicis C 1978 *Phys. Rev. B* **18** 4913
- [15] Coolen A C C 2002 *Markov Proc. Rel. Fields* (in press), preprint [cond-mat/0205262](#)
- [16] Crisanti A, Horner H and Sommers H-J 1993 *Z. Phys. B* **92** 257
- [17] Cugliandolo L F, Dean D S 1995 *J. Phys. A: Math. Gen.* **28** 4213
- [18] Challet D and Zhang Y-C 1998 *Physica A* **256** 514
- [19] Manuca R, Li Y, Riolo R, Savit R, University of Michigan Technical Report No. [pacs-98-11-001](#), [adap-org/9811005](#)
- [20] Eissfeller H and Opper M 1992 *Phys. Rev. Lett.* **68**, 2094